

## **General Disclaimer**

### **One or more of the Following Statements may affect this Document**

- This document has been reproduced from the best copy furnished by the organizational source. It is being released in the interest of making available as much information as possible.
- This document may contain data, which exceeds the sheet parameters. It was furnished in this condition by the organizational source and is the best copy available.
- This document may contain tone-on-tone or color graphs, charts and/or pictures, which have been reproduced in black and white.
- This document is paginated as submitted by the original source.
- Portions of this document are not fully legible due to the historical nature of some of the material. However, it is the best reproduction available from the original submission.

(NASA-CR-166589) DOUBLE ARCH MIRROR STUDY  
Final Report (Arizona Univ., Tucson.) 49 p  
HC A03/EF A01 USCL 131

884-31637

Unclass

63/37 20179

Optical Sciences Center  
University of Arizona  
Tucson, Arizona

## DOUBLE ARCH MIRROR STUDY

### FINAL REPORT

Prepared for:

NASA Ames Research Center  
Space Technology Branch 244-7  
Moffett Field, California 94035

NASA Grant No. 2-220

By:

Daniel Vukobratovich

Principal investigator:

Don Hillman

November 1983



## TABLE OF CONTENTS

INTRODUCTION . . . . .	.1
MIRROR MODIFICATION. . . . .	.6
MIRROR MOUNT . . . . .	18
TESTING. . . . .	23
CONCLUSION AND DISCUSSION. . . . .	34
REFERENCES . . . . .	40
APPENDIX . . . . .	41

## I. INTRODUCTION

The purpose of the double arch mirror study was to develop a method of mounting light-weight glass mirrors for astronomical telescopes that would be compatible with the goals of the Shuttle Infrared Telescope Facility (SIRTF). A 20-in. diameter double arch lightweight mirror previously fabricated at the Optical Sciences Center for NASA Ames Research Center was modified to use a new mount configuration. This mount concept was developed and fabricated at the Optical Sciences Center. Details of the mirror are available in Ref. 1; the development of the mount concept has been described in the "Preliminary engineering report" (March 1983) and "Engineering analysis report" (May 1983). Figures 1 and 2 provide details of the mounting concept. This report will deal with the modifications made to the mirror, fabrication of the mirror mount, and room temperature testing of the mirror and mount. An appendix is included to discuss the extension of the mirror and mount concept to a full size (40 in. diameter) primary mirror for SIRTF.

There were several areas of concern in the modification of the mirror. The first was possible figure change and degradation of mirror quality after removal of the integral mounting ring from the mirror back. This problem was addressed by testing the mirror figure before and after this operation. A second concern was the feasibility of machining sockets in the mirror's back. Use of expendable test blocks made of the same glass as the mirror (Corning Code 7940) allowed

ORIGINAL PAGE  
BLACK AND WHITE PHOTOGRAPH

ORIGINAL PAGE  
BLACK AND WHITE PHOTOGRAPH



Fig. 1. Front view of double arch mirror and mount assembly with translation stages to simulate cryogenic contraction of baseplate.

ORIGINAL PAGE  
BLACK AND WHITE PHOTOGRAPH



Fig. 2. Rear view of double arch mirror and mount assembly with translation stages to simulate cryogenic contraction of baseplate.

considerable practice and experience to be built up before tackling the mirror. Last, despite the favorable finite element model, there was some uncertainty about the stress in the socket area. Photoelastic tests of a full scale cross section plastic model reduced the uncertainty.

The only area that presented a potential problem in fabrication of the mirror mount were the tolerances on the titanium flexures. Experience has now shown that these tolerances can be held. However, the fabrication process is tedious and requires painstaking hand work.

The mirror and mount assembly were tested hanging upside down in the same orientation that will be used in the NASA Ames cryostat with a Shack interferometer. An attempt was made to simulate the cryogenic contraction of the aluminum baseplate. This was done by mounting the base of each flexure on a micrometer-controlled linear translation stage. This stage was used to move the base of each flexure radially to simulate differential thermal contraction of the baseplate. The mirror's optical figure was tested before translating the flexure bases. The translation stages were then set to simulate the cryogenic soak, and the mirror tested again. The translation stages were returned to their starting position and the mirror was tested a final time. In addition, the mirror was tested on edge, with its optical axis horizontal to ascertain the practicality of testing in this position.

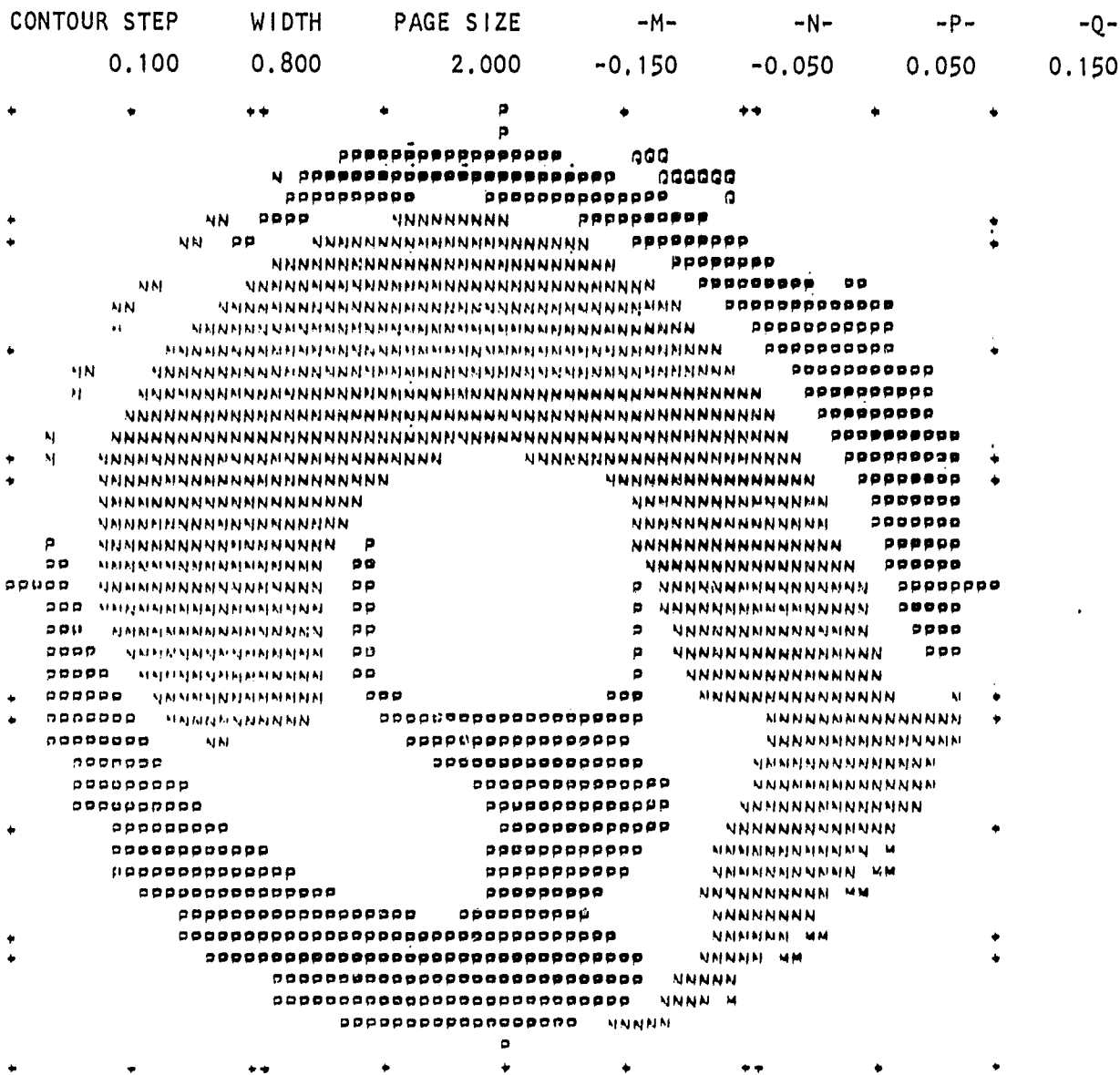
## II. MIRROR MODIFICATION

The double arch mirror was tested to determine its existing figure prior to modification. This test allowed a check to be made for figure change after modification. The test was performed by placing the mirror on its back (optical axis vertical). The mirror was placed on a styrofoam pad that provided continuous support against the back of the mounting ring. This pad also provided some vibration isolation. A Shack interferometer placed at the radius of curvature was used to produce interferograms of the optical figure. A folding flat was used to place the interferometer in a convenient horizontal location. To remove possible errors due to this folding flat, four interferograms were taken; after each interferogram was made the interferometer optics were rotated 90°. The actual interferograms were Polaroid prints. These prints were digitized manually and then analyzed using the FRINGE program. By using the four rotated interferograms, the FRINGE program removed the effect of the test optics.

The initial optical test results are shown in Figure 3. The RMS surface error was found to be 0.045 waves at 0.6328  $\mu\text{m}$ . The peak-to-valley error was found to be 0.297 waves. These results are of interest considering that the double arch mirror had not been tested in this mode previously. The double arch mirror when previously tested on its back on a three-point support had an RMS error of 0.081 waves. Of this error,



ORIGINAL PAGE IS  
OF POOR QUALITY



Residual Wavefront Variations over Uniform Mesh

PTS	RMS	MAX	MIN	SPAN	VOLUME
664.	0.045	0.125	-0.172	0.297	0.507

Units = Waves at 0.6328  $\mu$ M.

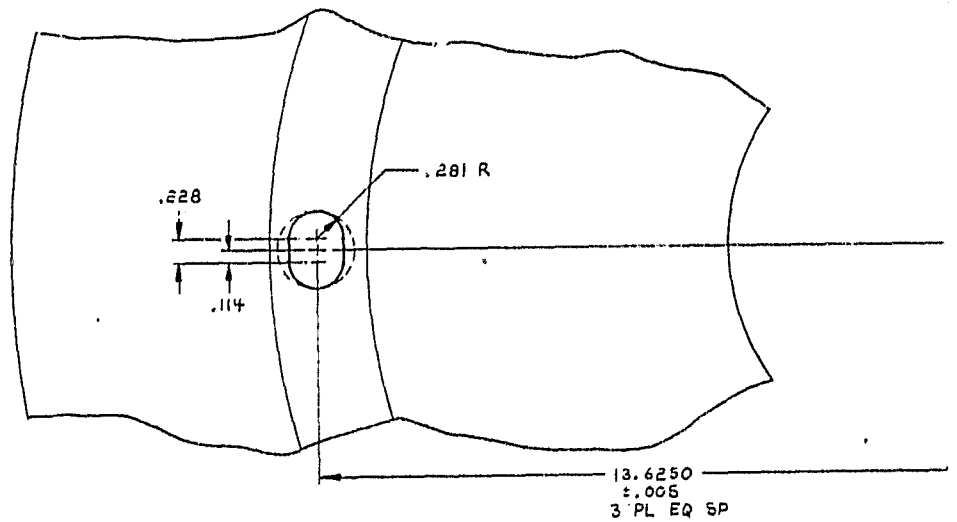
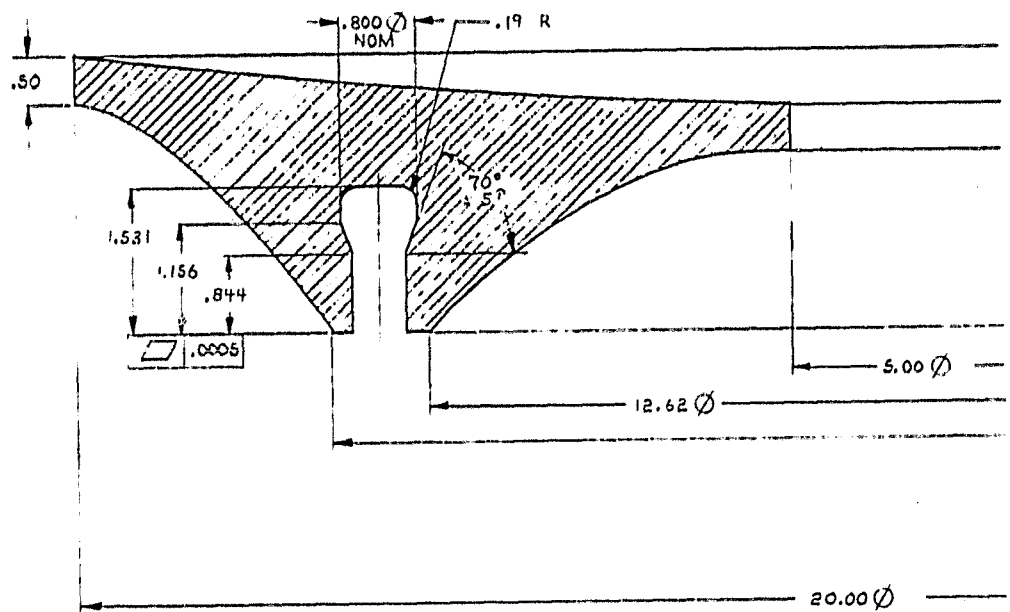
Fig. 3. Mirror figure as received. Mirror lying on its back, continuous support on mounting ring.

0.037 waves were 36 terms due to the effect of the support. Simple subtraction of the 36 term would give an RMS of 0.044 waves, which is within 2.25% of the continuous support result.<sup>2</sup>

Following testing, the mirror was prepared for modification. An aluminum alloy tooling plate disk 24 in. in diameter and 0.75 in. thick was used as a tooling fixture. The optical surface of the mirror was protected by covering it with wax. The mirror was waxed down to the aluminum plate, optical surface down. During the waxing process, the optical axis of the mirror was made coincident with the rotational center of the aluminum plate.

The tooling plate and mirror assembly were mounted to the spindle of a conventional glass generator machine. The rotational axis of the tooling plate was coincident with the axis. A diamond impregnated grinding wheel machined away the mirror's mounting ring as the spindle rotated the mirror. The operation was halted when 1.00 in. of the mounting ring was removed. This left a flat surface on the back of the mirror (Fig. 4).

Putting the sockets into the back of the mirror required special diamond tooling. Due to the slenderness of the special tooling, the use of a high-strength steel as a base for the diamonds was required. Use of a high-strength material will not alter the dynamic behavior of the tool; but it will prevent permanent deformation or even failure from



FOLDOUT FRAME

ORIGINAL PAGE IS  
OF POOR QUALITY

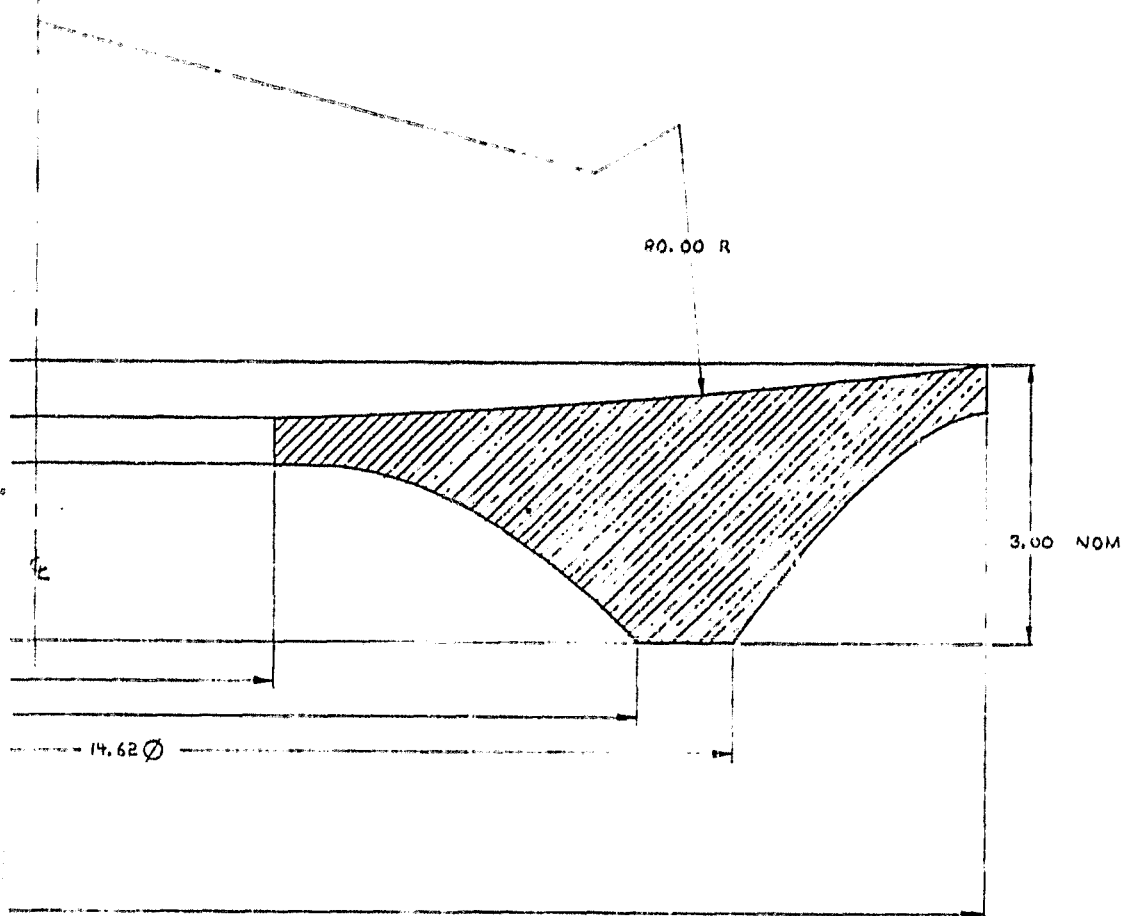


Figure 4. Cross section of modified 20-in. diameter double arch mirror.

EOLDOUT FRAME 2

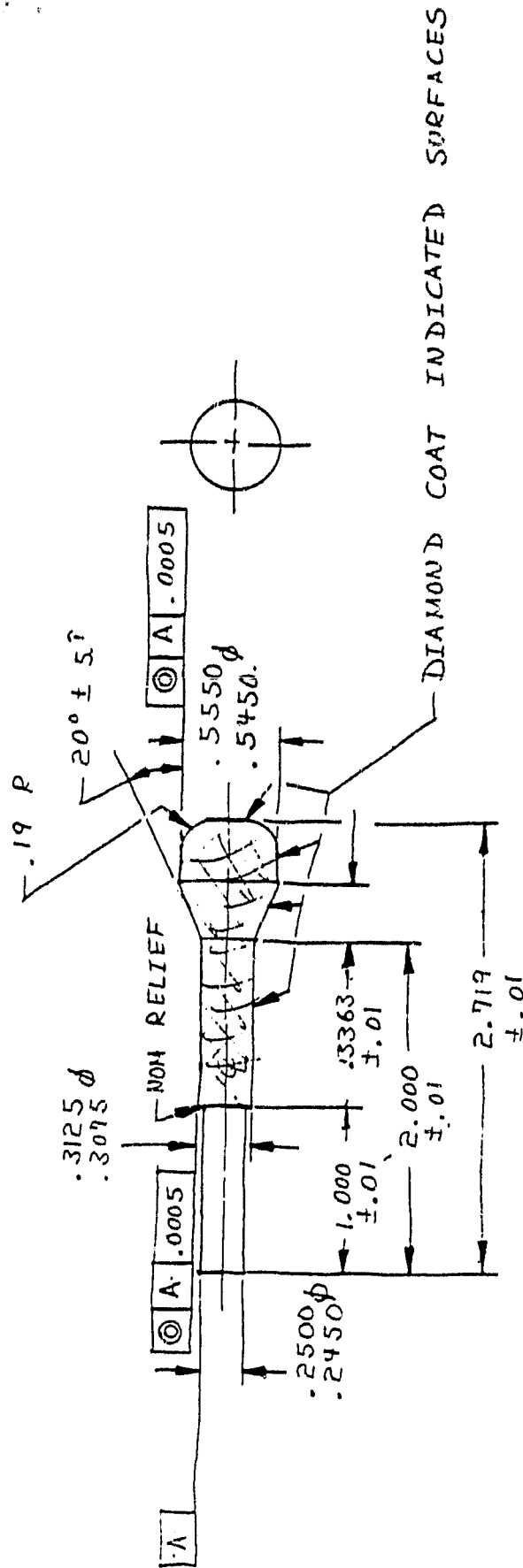
				TOLERANCES (EXCEPT AS NOTED)		OPTICAL SCIENCES CENTER UNIVERSITY OF ARIZONA			
				DECIMAL INCHES 3 PLACES 0.01 0.03		DESCRIPTION CROSS SECTION OF DOUBLE ARCH UNIFORM STRESS SUBSTRATE			
				MATERIALS 2		TITLE NASA/AMES 20" LIGHTWEIGHT MIRROR			
1 MOUNTING RING REMOVED, SOCKET				CHG 83 SV		SCALE FULL			
REV.	DESCRIPTION	DATE	BY	APPROVED BY	DATE	APPROVED BY	DATE	REVISION NUMBER	REV.
				SV	08/8				
				SV	08/8				
FINAL APPROVED		DATE		APPROVED BY		DATE		REVISION NUMBER	

occurring. To minimize the time needed to make the tooling, 17-4 PH stainless steel, in condition H 1150-M was used. This material is a precipitation hardening, magnetic stainless steel with a yield strength of 75,000 psi.<sup>1</sup> This material was machinable at full strength, thus no heat treatment was needed. Conversations with Diachrome, the diamond tool maker, had indicated that for proper adhesion of the diamond, a magnetic steel was required.

Several special tools were made. A conventional core drill was made for initial coring of the socket. A simple diamond coated cylinder was made for elongating the socket hole. Another set of tooling was made for finishing the conical area of the socket (Fig. 5). This last set of tooling consisted of three identical tools, each coated with a different grade of diamond. The grades were 120, 220, and 400. It was intended to do most of the socket cutting with the coarse grade, smooth up the cut with the number 220 and produce the finished surface with the number 400 coated tool.

As a first step in fabricating the socket, the mirror and tooling plate assembly were transferred from the generator to a rotary table mounted on a milling machine. The rotary table was used as an aid in locating the position of the three sockets.

The tooling plate and mirror were moved atop the rotary table until the center of rotation of the rotary table was coincident with the



3 REQ'D

MATL: 17-4 PH CRES STL  
COND H50-M

Fig. 5. Special diamond tool for cutting conical socket surfaces.

future center of the socket. This involved decentering the work piece relative to the rotary table. The diamond coated core drill was used to core into the mirror back to a depth slightly less than the final depth of the socket. The glass plug was then broken out of the back of the mirror.

The bottom of the resulting hole was cleaned with a steel plug tool and loose abrasive. An attempt was made to perform this operation using the cylindrical diamond tool. This failed, due to lack of a good bond between the steel and the diamond, as well as rapid wear at the center of rotation of the tool.

The cylindrical tool did prove useful in the next operation, elongating the hole. The tool was rotated in the chuck of the milling machine while the horizontal motion of the milling table was used to decenter the tool. This combination of motions was able to produce the elongated hole or slot needed to insert the clamp into the socket.

The final operation was cutting the conical socket surfaces. The special conical tooling mentioned previously was used. The tool coated with the coarsest grade of abrasive, number 120, was chucked up in the milling machine. The horizontal milling table was used to bring the mirror and tooling plate and the rotary table carrying them into a position such that the center of rotation of the chuck was coincident with the center of the socket and the center of rotation of the rotary

table. The mirror was decentered an amount equal to half the quantity of the internal diameter of the conical socket less the maximum outer diameter of the tool. The tool was rotated by the milling machine chuck as the rotary table rotated the mirror under it. The tool center traced a circle whose center was coincident with the socket center. As the tool rotated about this circle, its contact point was tangent to the internal diameter of the socket. In this way, the conical socket area was formed.

It had been hoped to cut all the conical sockets with the 400 grade tool. Rapid wear of the diamond coating precluded this, forcing the use of the coarse number 120 grade tool. Part of the wear problem was due to lack of adhesion of the diamonds to the 17-4 PH stainless steel of the tool. This suggests that future tooling should be made of a high strength carbon tool steel. Such a tool would be more expensive and time consuming to make, but would allow a better surface finish to be attained.

The described operation was performed three times, once for each socket. To gain experience in the procedure, Edward Strittmatter, the Optical Sciences Center optician performing the work, practiced on several glass blocks. All cutting operations were performed on these expendable blocks and complete sockets were made. When confidence had been gained, as a last practice step, a complete socket was generated in glass from the cored-out plug from the mirror. This insured that all



problems with the tooling and process were solved prior to making any cuts on the glass. A useful byproduct was the creation of a complete socket in a block of Corning Code 7940 glass from the original mirror blank. This makes several further avenues of research open that will be discussed in the conclusion of this report (Figs. 6 and 7).

After socket fabrication was complete, the mirror was removed from the tooling plate, and the protective wax removed from the optical surface. The weight of the mirror following modification was 34 lbs. The mirror was cleaned, and tested to see if the optical figure had changed. The optical test set-up was identical to that used earlier, as was the test procedure. The results of this test can be seen in Fig. 8. The RMS surface error was now 0.017 waves, and the peak-to-valley error was 0.121 waves. The surface figure had changed from the original RMS and peak-to-valley figures. The improvement was by a factor of 2.6. Since the original fabrication of the double arch mirror had included an acid-etch stress relief, it is difficult to understand what led to the figure improvement. It is possible that lack of flatness of the back of the mounting ring could have led to excessive deformation, although the use of the compliant rubber pad for support should have eliminated this effect. The improvement is of the same order as the measurement error and is therefore somewhat suspect.

Fabrication of the socket did not include a final acid-etch stress relief. This step was eliminated for fear of possible damage to the

ORIGINAL PAGE  
BLACK AND WHITE PHOTOGRAPH.

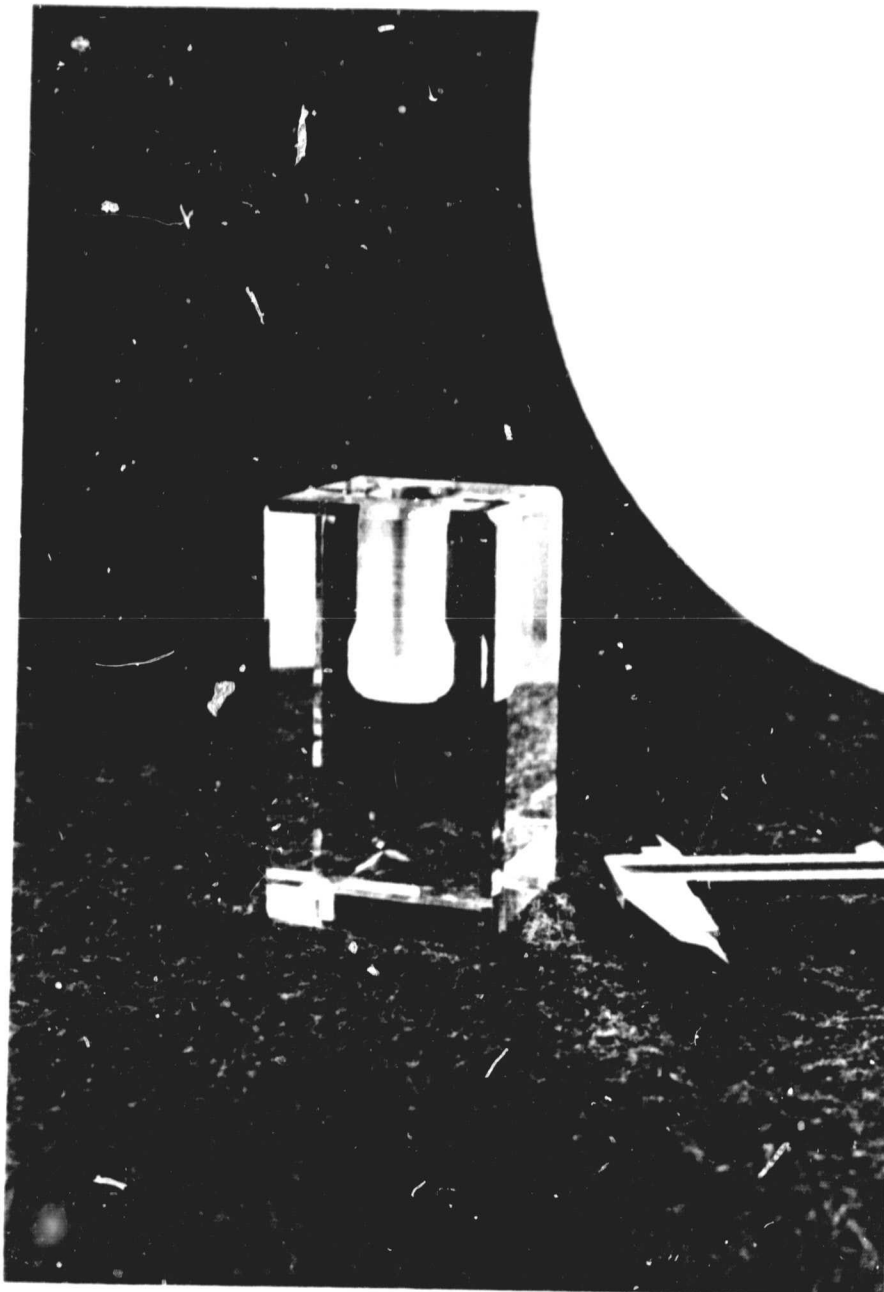


Fig. 6. Side view of practice socket block.

ORIGINAL PAGE  
BLACK AND WHITE PHOTOGRAPH

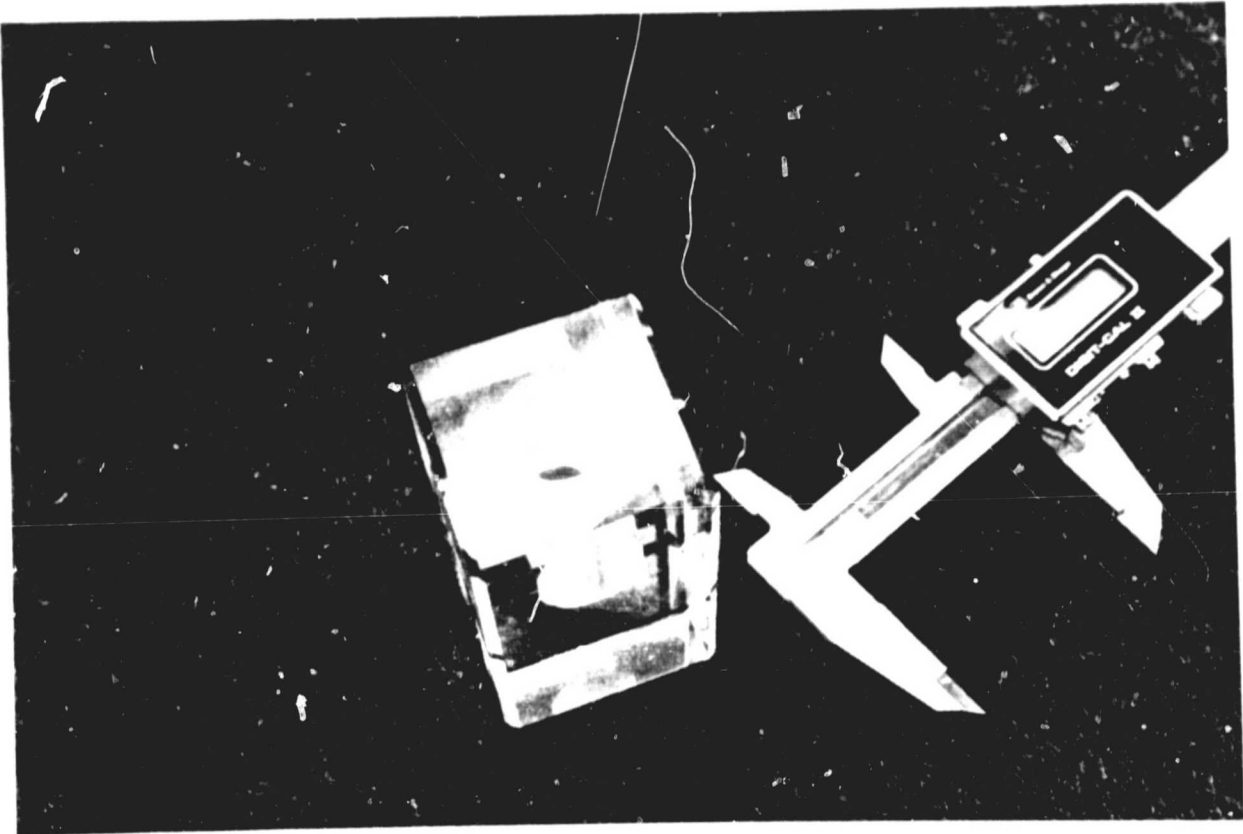


Fig. 7. Top view of practice socket block.

ORIGINAL PAGE IS  
OF POOR QUALITY

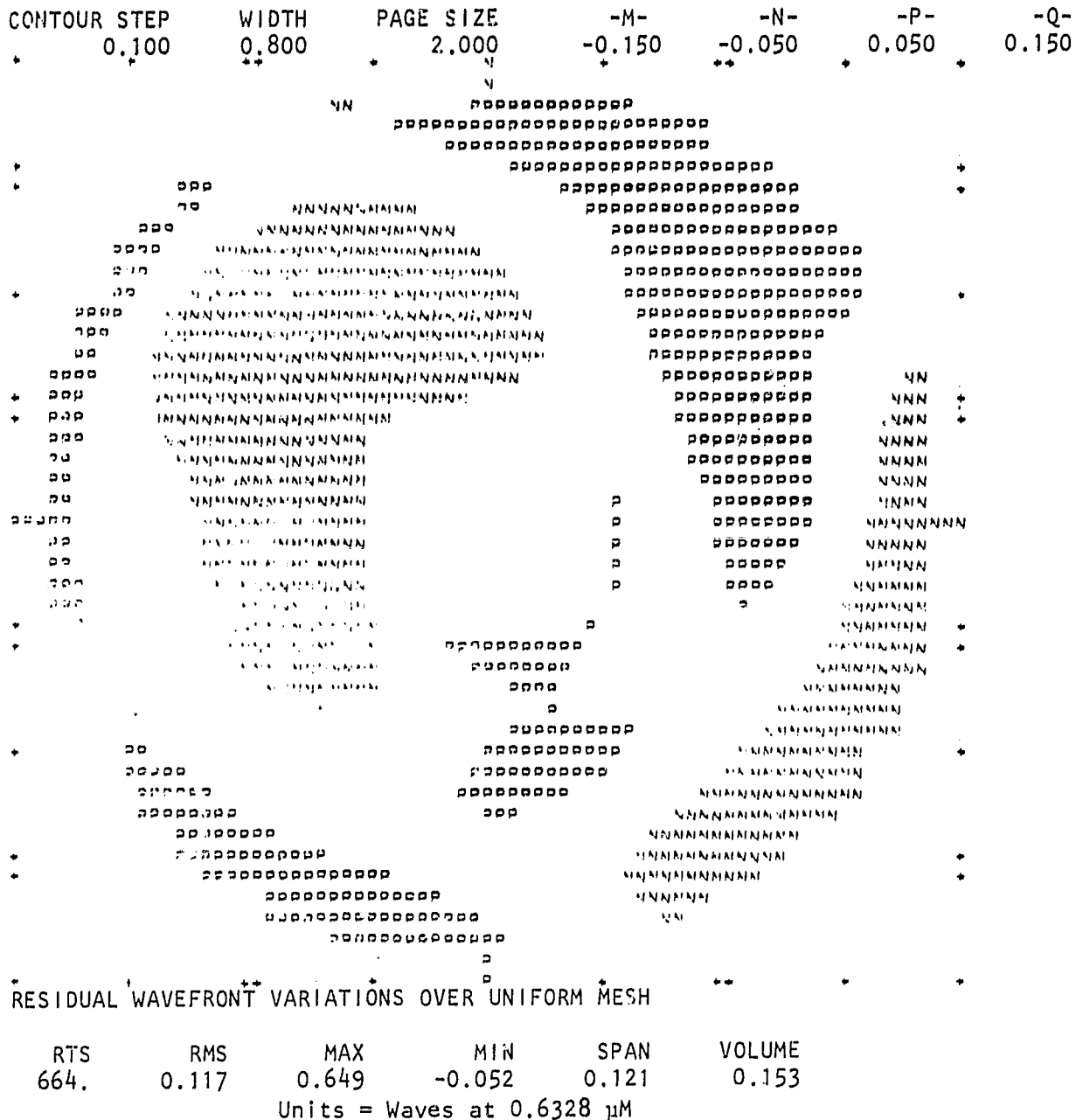


Fig. 8. Mirror figure after modification. Mirror on its back, back continuously supported.

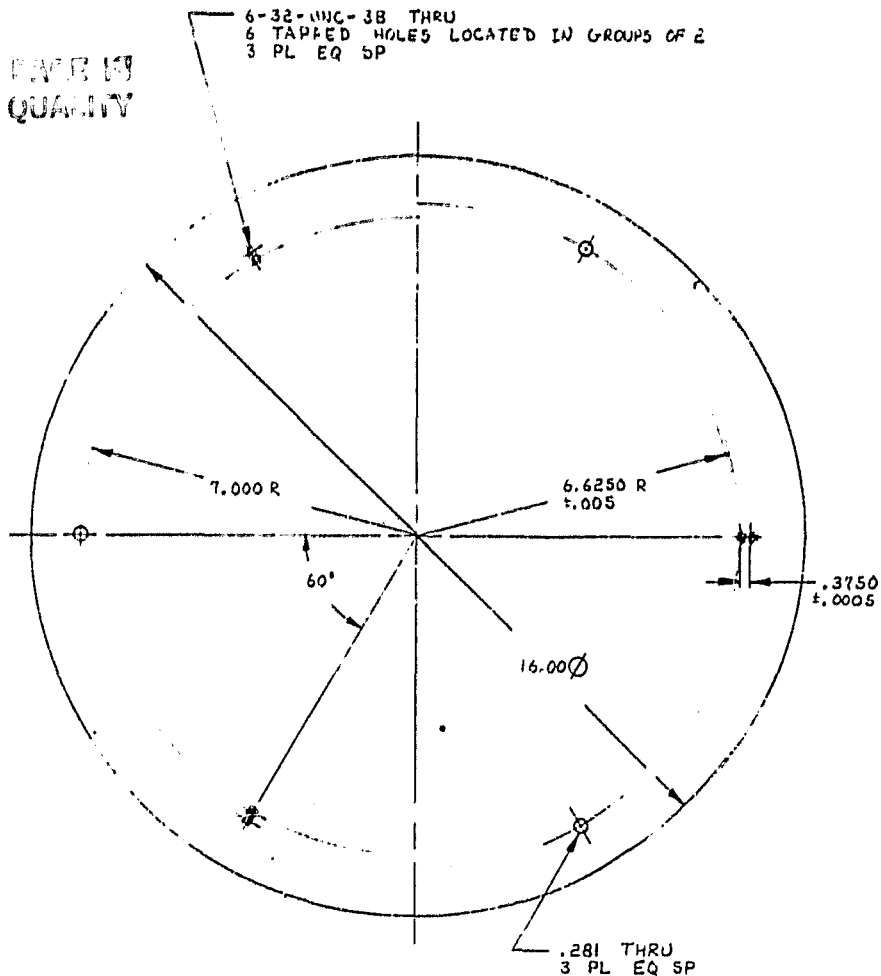
optical surface and because of the rough texture of an acid-etched surface. Further grinding would have been required to smooth the acid-etched surface, which would have partially defeated the purpose of such a stress relief. In a future similar project, an acid etch could be performed on the mirror after all generating work, including the sockets, had been performed prior to polishing the optical surface. This would minimize the risk, but would still leave some residual stress and damage owing to the need for a final fine grind on the socket surfaces.

### III. MIRROR MOUNT

Construction of the mirror mount parts did not pose any serious problems and was accomplished using conventional shop techniques (Fig. 9). Some concern had been expressed earlier in regards to fabrication of the titanium flexures. Two problems were envisioned: holding the required tolerances and the possible "springing" of the flexure during fabrication. The parallelism tolerance for the top and bottom of the flexure was 0.0005 in. The parallelism tolerance of the flexure blades was 0.001 in. These tolerances were derived from the analysis performed in the "Engineering analysis report" dated May, 1983. A high surface finish, number 16 on the broad side of the flexure blades, was specified to reduce possible crack formation at cryogenic temperatures. A very generous 0.125 in. transition radius between the flexure blades and flexure ends reduced stress concentration.

PART 1: FLEXURE

ORIGINAL PART IS  
OF POOR QUALITY



1 REQD  
MATL: .25 THICK 6061 CAST AL ALLOY TOOLING PLATE

PART 4: BASEPLATE

SCALE: 1/2 X

Figure 9. Mirror mount details.

				OPTICAL SCIENCES CENTER UNIVERSITY OF ARIZONA			
				DESCRIPTION MIRROR MOUNT & DETAILS			
				TITLE NASA DOUBLE ARCH MIRROR			
				SCALE FULL (EXCEPT AS NOTED)			
REV.	DESCRIPTION	DATE	BY	DESIGNED BY DATE (CHECKS)	APPROVED BY DATE (CHECKS)	DATE	REVISION NUMBER
							060985-1
FINAL ASSEMBLY		TEST ASSEMBLY		ANGULAR ±0° 30' (EXCEPT AS NOTED)	DATE (CHECKS)	DATE	REV.

In actual fabrication, no problem was encountered in holding the parallelism tolerances. The Ti-6Al-4V ELI alloy had been furnished in plate form. It was found to be stable and not prone to "springing" despite removal of gross amounts of material. Obtaining the desired surface finish also proved straightforward. Since the Optical Sciences Center does not have a jig grinder, it was necessary to perform considerable handwork on the flexures following milling to obtain the desired finish.

The current flexure design represents the limit in terms of tolerances that might be expected to come out of the Optical Sciences Center fabrication shop. This does not mean that a more tightly toleranced flexure is not possible. What it does mean is that tighter tolerances would require better facilities and a greater risk than the existing design. Analysis has shown that thinner flexure blades have better performance. Charles Brown, the head of the Optical Sciences Center Instrument Shop, is ready to try a flexure with blades as thin as 0.030 in. Should further work be performed on this flexure concept, it is strongly suggested that an attempt be made to further develop the state of the art in fabrication. In particular, thinner, higher tolerance flexures should be attempted. On the other hand, decreasing the tolerances by a factor of two would reduce fabrication time by at least a third. More complex flexure configurations, such as might be required to remove baseplate deformations, could take advantage of this.



The remainder of the mirror mount components did not present any particular problem. Two modifications were made to the original mount design. The contact surfaces of the clamps were gold coated, and translation stages were placed under the base of the flexures, between the flexure and baseplate.

The gold coating on the clamps was put on using optical coating techniques in a coating chamber. The coating thickness was on the order of 0.002 in. Adhesion was poor; the coating could literally be rubbed off using a fingernail. Gold was used instead of silver since prior experience had shown silver to have tarnishing and adhesion problems. The gold coating was intended to act as a surface lubricant and to add some compliance in the contact area. Disassembly of the mount following testing revealed that the primary role of the gold coating was to indicate the amount of contact achieved between the clamp and the socket. That is, the better the contact, the more gold that came off the clamp. It is suggested that either the gold coating be eliminated from future designs, or that an alternate coating technology be developed.

The translation stages were Delton Catalogue No. 401 positioning slides. These have a load capacity of 20 lbs each, and a total travel range of 0.50 in. A micrometer drive is provided with a positioning accuracy of 0.001 in. The accuracy of travel as specified by the manufacturer is 0.0005 in. per inch of travel. The direction of translation for these slides was radial with respect to the baseplate

center. Displacing the slides 0.029 in. radially inwards simulated contraction of the baseplate as temperature was reduced to 10°K. This allowed the flexure performance to be evaluated at room temperature. It must be emphasized that the translation stages should not be used at cryogenic temperatures and should not remain a permanent part of the mirror mount assembly.

All mounting hardware on the mirror mount was stainless steel. Stainless was used in place of conventional carbon steel to gain increased fracture toughness at cryogenic temperatures.' Although carbon steel fasteners might be acceptable given the very benign test environment, they would be totally unsuited for space use in a dynamic environment.

Finally, although designed to survive emergency landing conditions aboard the space shuttle, the mirror and mount assembly must be considered precision optical components and treated as such. Dropping a flexure on the floor would ruin it. A sharp blow to the assembly might misalign the system to the point where it would not perform as desired. Unlike glass, metal has a "memory" and does not necessarily reveal fatal damage to the unaided eye. Rigorous monitoring of assembly and handling procedures is therefore in order.

#### IV. TESTING

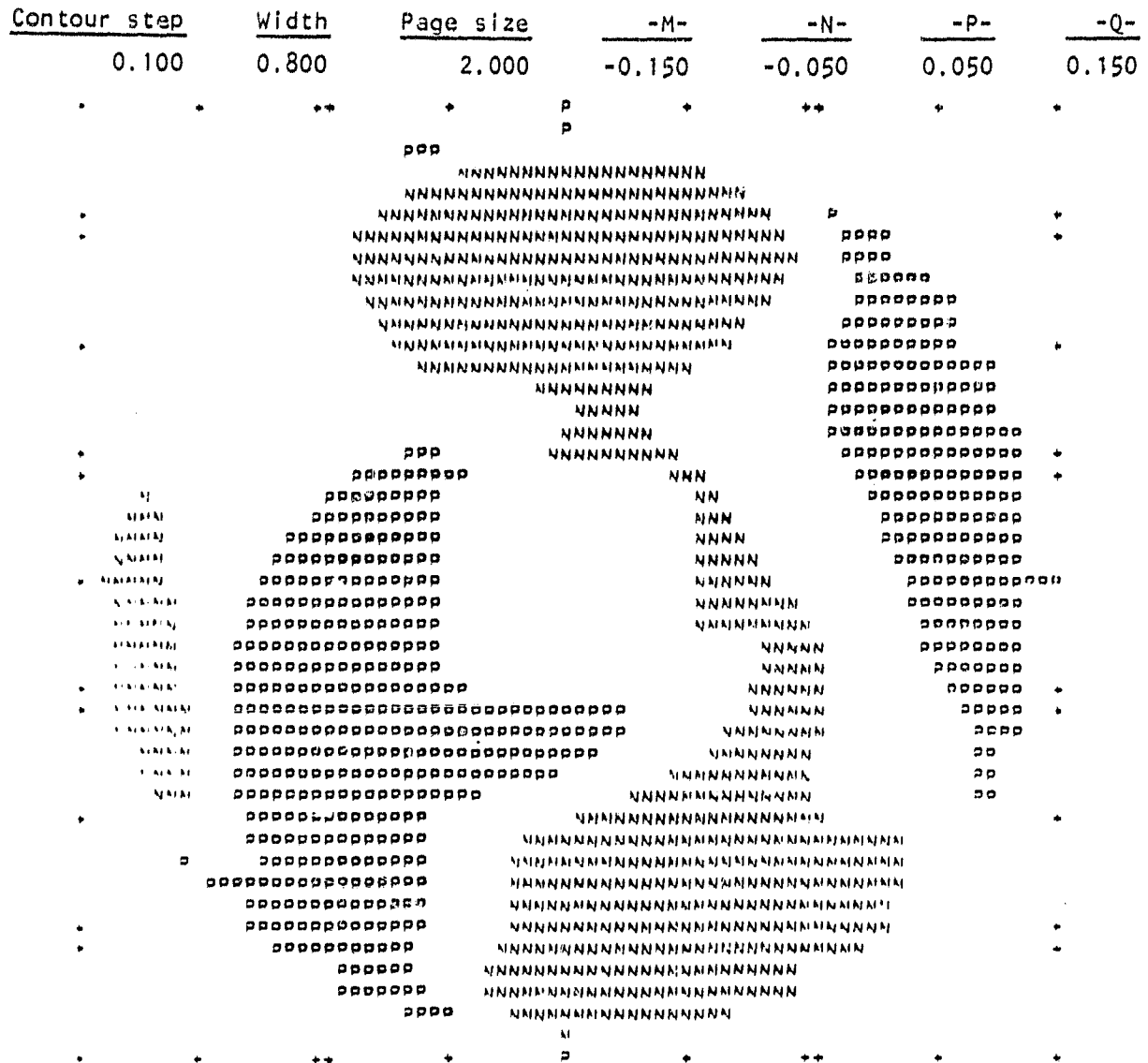
Initially, the mirror and mount assembly were mounted upside down, optical surface facing down (optical axis vertical) to simulate the NASA Ames cryostat. In this position, the mirror was first tested in the unstressed position, then the translation stages were used to simulate cryogenic contraction of the baseplate and resultant stress on the assembly. The translation stages were returned to the starting position and the mirror figure tested a third time. This established repeatability of the test. The same series of unstressed and stressed tests were also performed with the mirror in the "on edge" position (optical axis horizontal). In addition, a plastic full-scale model of the flexure, clamp, and socket were also tested for stress photoelastically.

The upside down test was very similar to the test performed to establish the figure of the mirror as received. The mirror and mount were suspended upside down from a steel scaffold. The baseplate of the mirror mount was secured to the scaffold by three 0.25-20 socket head screws with spherical washers between the baseplate and scaffold. The spherical washers prevented lack of flatness in the scaffold from bending the baseplate. A Shack interferometer was placed at the radius of curvature. A folding flat was used to place the interferometer in a more convenient horizontal position. The fringes were recorded on Polaroid film and manually digitized. As before, four sets of

interferograms were made, with the test optics being rotated  $90^\circ$  between each set. This allowed the FRINGE program to remove errors due to the test optics. Fiducial marks were added to the optical surface of the mirror for reference during digitizing. Vibration and air turbulence were serious problems during testing. To reduce vibration, the steel scaffold originally used was replaced by a very heavy steel scaffold fabricated from 8 in. channel and 6 in. square steel tubing. This scaffold was normally used to support 72 in. mirrors and offered better stability. In spite of this, better isolation from vibration and turbulence would have been desirable.

Results of the first optical test are shown in Fig. 10. The translation stages are in a neutral position, and the mirror and mount are unstressed. It is seen that the RMS surface error is 0.022 waves at  $0.6328 \mu\text{M}$ . The peak-to-valley error is 0.114 waves. The mirror does not display any gross three-fold symmetry imposed by the three-point support.

The translation stages were then driven 0.029 in. to simulate a cryogenic contraction of the aluminum baseplate. This corresponded to a  $10^\circ\text{K}$  final temperature. The results of this test are seen in Fig. 11. The RMS surface error is 0.017 waves and the peak-to-valley error is 0.109 waves. Again, there is no apparent print-through of the three support points.



Residual wavefront variations over uniform mesh:

PTS	RMS	Max.	Min.	Span	Volume
664.0	0.022	0.057	-0.057	0.114	0.168

Units = Waves at 0.6328  $\mu$ m

Fig. 10. Mirror under test upside down, unstressed.

# ORIGINAL OF POOR QUALITY

Contour step	Width	Page size	-M-	-N-	-P-	-Q-
0.100	0.800	2.000	-0.150	-0.050	0.050	0.150



Residual wavefront variations over uniform mesh:

PTS	RMS	Max.	Min.	Span	Volume
664.0	0.017	0.061	-0.048	0.109	0.142

Units = Waves at 0.6328  $\mu$ M

Fig. 11. Mirror under test upside down, stressed.

The translation stages were returned to their starting positions and a third test performed. This test result is shown in Fig. 12. The RMS surface error is 0.017 waves, and the peak-to-valley span is 0.114 waves. In this test, again no obvious effect of the three point support is visible.

From previous experience with this mirror and test configuration,<sup>2</sup> differences of 0.02 waves RMS and 0.15 waves peak-to-valley may be considered real. The maximum RMS change observed was 0.005 waves and the maximum peak-to-valley change was 0.005 waves. Thus the simulated cryogenic soak effect cannot be said to have been measured. A finite element model was used to predict the change in RMS surface figure in the mirror in going from room temperature to 10°K. The results of this model indicated that the figure would change 0.002 waves RMS. This is a factor of ten smaller than the sensitivity of the test apparatus. It is not therefore surprising that the simulation showed virtually no change. A more sensitive test is obviously required.

The mirror was also tested with its axis horizontal. The baseplate was bolted to a right angle bracket to hold the mirror in an "on edge" position. One flexure was oriented to be at the top of the mirror. The optical test was performed using a Zygo interferometer. Both interferometer and mirror were placed on a common granite surface plate for stability. Lack of space on the surface plate required a folding flat in the optical path. Due to the nature of the Zygo interferometer,

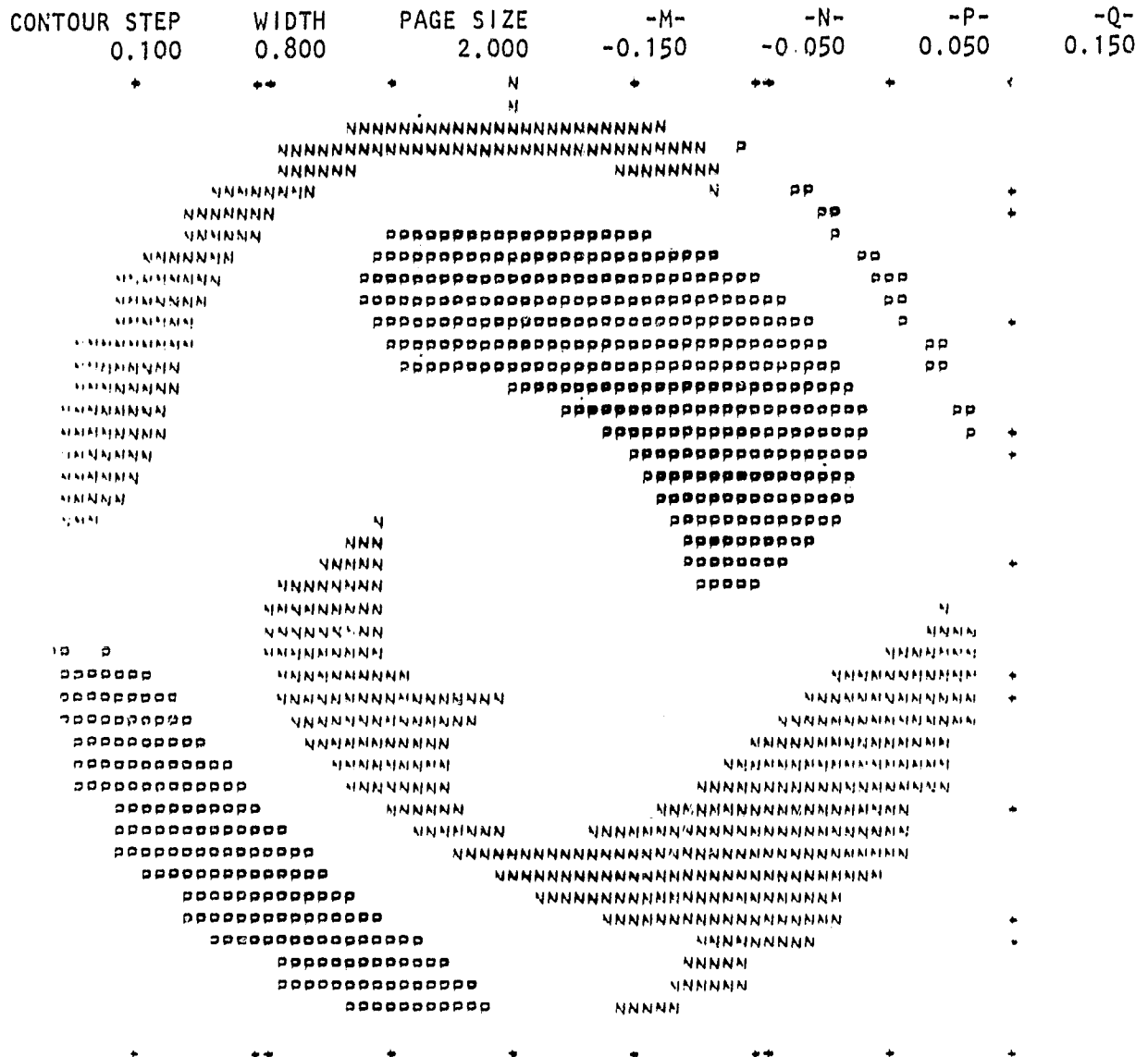


Fig. 12. Mirror under test upside down returned to unstressed condition.

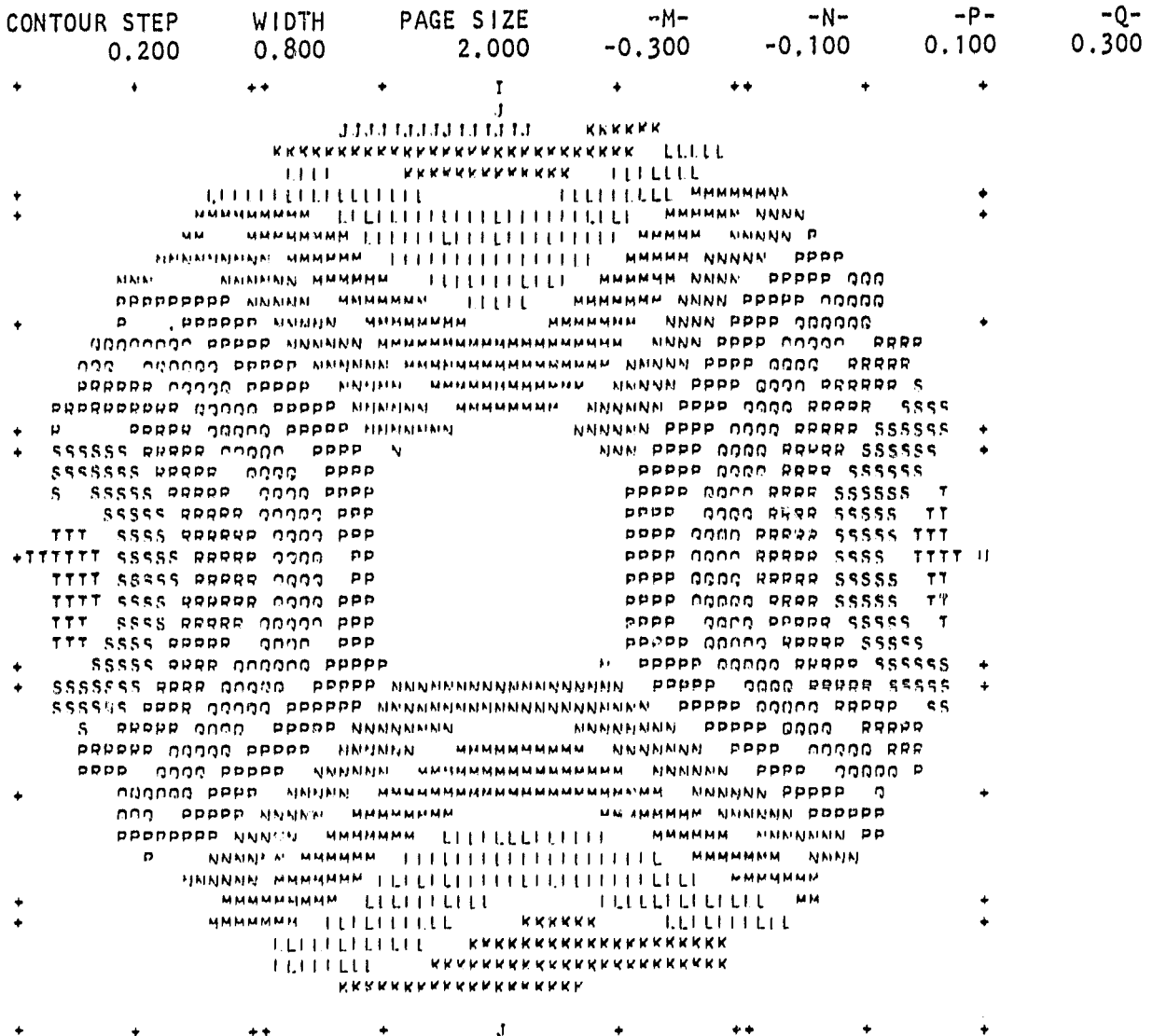


rotation of the test optics was not possible. Vibration and air turbulence were serious problems. The interference fringes were displayed on a TV monitor and recorded on Polaroid film. The interferograms were manually digitized and evaluated using the FRINGE program. It was not possible to remove the effects of the test optics.

The mirror and mount were first tested in the unstressed condition with the translation stages in the neutral position. The resulting surface figure is shown in Fig. 13. The RMS surface error was 0.453 waves at 0.6328  $\mu\text{M}$ . The peak-to-valley error was 2.113 waves. A very strong astigmatic component dominates this result.

The translation stages were then adjusted as in the upside down test to simulate a cryogenic contraction of the baseplate. The results are shown in Fig. 14. The RMS surface error was 0.441 waves and the peak-to-valley error was 2.165 waves. The astigmatism is obviously dominant and virtually unchanged from the unstressed condition.

Finally, the translation stages were returned to their starting position and the mirror tested again. This result is shown in Fig. 15. The RMS surface error was 0.449 waves, and the peak-to-valley error 1.951 waves. The astigmatism pattern appears again, apparently unchanged.



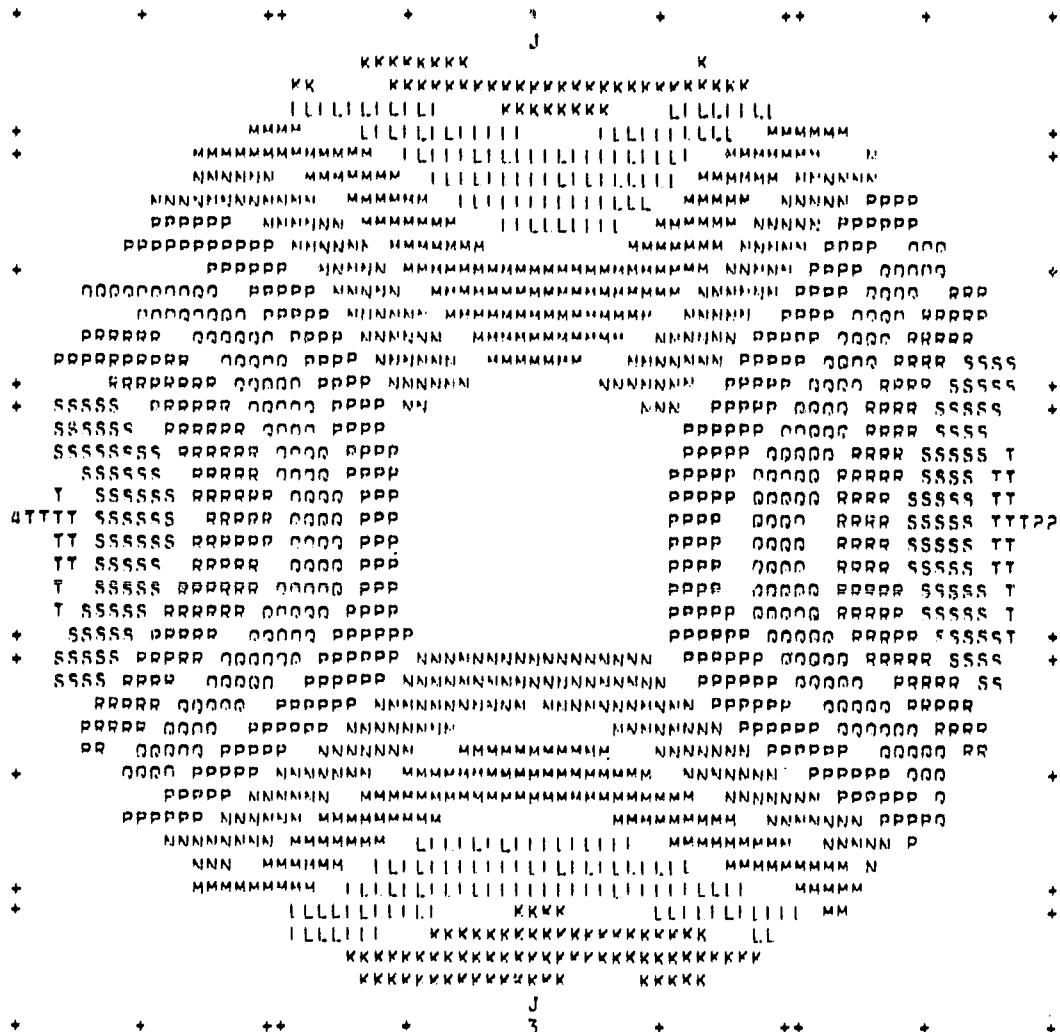
Residual wavefront variations over uniform mesh.

PTS	RMS	MAX	MIN	SPAN	VOLUME
664.	0.453	1.057	-1.056	2.113	3.115

Units = waves @ 0.6328  $\mu$ M.

Fig. 13. Mirror on edge test, unstressed.

CONTOUR STEP	WIDTH	PAGE SIZE	-M-	-N-	-P-	-Q-
0.200	0.800	2.000	-0.300	-0.100	0.100	0.300



Residual surface variations over uniform mesh.

PTS	RMS	MAX	MIN	SPAN	VOLUME
664.	0.441	0.076	-1.039	2.165	3.212

Units = waves at 0.6328  $\mu$ M.

Fig. 14. Mirror on edge test, stressed.

CONTOUR STEP	WIDTH	PAGE SIZE	-M-	-N-	-P-	-Q-
0.200	0.800	2.000	-0.300	-0.100	0.100	0.300

```

+      +      ++      +      J      +      ++      +
      KKKKKKKK  TJ.TJJ.TJJ  KK
      LLLL.LL  KKKKKK  TJ.TJJ  KKKKKK  LL
      MM  LLLL  KKKKKKKK  KKKKKKKK  LLL
+      MMMMMMMM  LLLL.LL  KKKKKKKKKKKKKKKKKKK  LLLL.MMMM  +
+      NNNNNN  MMMMM  LLLL.LL  KKKKKKKKKKKKKK  LLLL.MMMMMNNNN  +
      NNNNNN  MMMMM  LLLL.LL.LL.LL  LLLL.LL.LL  MMMMMMMN  P
      PPPP  NNNNN  MMMMMMM  LLLL.LL.LL.LL.LL.LL  MMMM  NNN  PPP  Q
      PPPPPPP  NNNNNN  MMMMMMMMM  LLLL.LL  MMMMMMMM  NNN  PPP  QQQQ
      PPPPP  NNNNNN  MMMMMMMMMMMMMMMMMMMMMMMMMMMMMMM  NNNN  PPP  QQQ  R
+      QQQ  PPPPPP  NNNNNNNN  MMMMMMMMMMMMMMMMMMMMMMMMMMM  NNNN  PPP  QQQRRR  +
      QQQQQQQ  PPPPPP  NNNNNNNNN  MMMMMMMMMMMMMMM  NNNNNN  PPP  QQQRRR  S
      P  QQQQQQ  PPPPPP  NNNNNNNNNN  NNNNNNNNNN  PPP  QQQRRR  SSS
      PPP  QQQQQQ  PPPPPP  NNNNNNNNNNNNNNNNNNNNNNNNNNNNN  PPP  QQQ  RRR  SSSS
      PPPPPP  QQQQQQ  PPPPPP  NNNNNNNNNNNNNNNNNNNNNNNNNNN  PPP  QQQ  RRR  SSSS
+      PPPP  QQQQQ  PPPPPP  NNNNNNNNNNNNNNNNNNNNNNNNNNN  PPPP  QQQ  RRRSSSS  TTT  +
+      SS  PPPPPP  QQQQQ  PPPPP  NNN  NN  PPPPP  QQQQQRRR  SSS  TTTT  +
      SSSS  PPPPPP  QQQQ  PPPPP  PPPPPP  QQQ  RRR  SSS  TTTT
      SSSSS  PPPPPP  QQQQ  PPPPPP  PPPPPP  QQQ  RRRSSS  TTTT
      SSSSSS  PPPPPP  QQQQ  PPPPPP  PPPPPP  QQQ  RRRSSS  TTTT
      SSSSSS  PPPPPP  QQQQ  PPPPPP  PPPPPP  QQQ  RRRSSS  TTTT
4TT  SSSSSS  RRRR  QQQQ  PPPPPP  PPPPPP  QQQ  RRR  SSSSTTTT
      T  SSSSSS  RRR  QQQQ  PPPPPP  PPPPPP  QQQQRRR  SSS  TTTT
      T  SSSSSS  RRR  QQQQQ  PPPPPP  PPPPPP  QQQQ  RP  SSS  TTTT
      T  SSSSSS  RRR  QQQQQ  PPPPPP  PPPPPP  QQQQ  RRRSSSS  TTT
      SSSSS  RRRR  QQQQ  PPPPP  PPPPPP  QQQ  RRR  SSSS  TT
+      SSSSSS  RRRR  QQQQ  PPPPPPP  PPPPPPPPPPP  QQQQ  RRR  SSSS  +
+      SSSSSS  RRRR  QQQQQ  PPPPPPP  PPPPPPPP  QQQ  RRRR  SSSSS  +
      SSSSS  RRRR  QQQQ  PPPPPP  NNNNNNNNNNNNNNNNNNN  PPPPPP  QQQ  RRRR  SSSS
      S  RRRR  QQQQQ  PPPPPP  NNNNNNNNNNNNNNNNNNNNNNNNNNN  PPP  QQQ  RRRR
      RRRR  QQQQQ  PPPPP  NNNNNNNNNNNNNNNNNNNNNNNNNNNNN  PPPPP  QQQQ  RRRP
      PPPPP  QQQQQ  PPPPP  NNNNNNNNNNNNNNNNN  NNNNNNNNNNN  PPPP  QQQQ  RP
+      QQQQQ  PPPPP  NNNNNNNN  MMMMMMMMMMMMMMM  NNNNNNN  PPPPP  QQQ  +
      QQQQ  PPPPP  NNNNNN  MMMMMMMMMMMMMMMMMMMMMMMMMMMMMMM  NNNNN  PPPPP  Q
      QQ  PPPPP  NNNNNN  MMMMMMMMMMMMMMM  MMMMMMMMMMMMMMM  NNNNN  PPPPP
      PPPPP  NNNNN  MMMMMMMM  LLLL.LL.LL.LL.LL  MMMMMMMM  NNNN
      NNNNN  MMMMM  LLLL.LL.LL.LL.LL.LL.LL.LL  MMMMM  A
+      NNNN  MMMMM  LLLL.LL.LL.LL  LLLL.LL.LL  MMMM
+      MMMMMMM  LLLL.LL  KKKKKKKKKKKKKKKKKKK  LLLL.LL
      LLLL.LL  KKKKKKKKKKKKKKKKKKKKKKKKKKKKK
      LLLL  KKKK  KKK  TJ.TJJ  KKKKK
      KKKKKKK  TJ.TJJ.TJJ.TJJ.TJJ.TJJ
      J
+      +      ++      +      J      +      ++      +

```

Residual surface variations over uniform mesh

PTS	RMS	MAX	MIN	SPAN	VOLUME
664.	0.449	0.956	-0.995	1.951	2.935

Units = waves @ 0.6328  $\mu\text{m}$

Fig. 15. Mirror on edge test, return to unstressed.

The maximum change in the RMS was 0.012 waves. The maximum peak-to-valley error change was 0.214 waves. Since it was not possible to remove the effects of the test optics, these results cannot be considered as accurate as the upside down test. Even by the standards of this test, only the peak-to-valley error change has meaning. It is suggested that this change should be taken with some skepticism.

The primary figure error observed was astigmatism. This was induced by the flexures. Since the flexures are oriented at  $60^\circ$  relative to the gravity vector direction, the support reaction also produces a force at right angles to the gravity vector. Since there are two flexures supporting the weight of the mirror (the upper flexure has its compliance direction in the same direction as the gravity vector) and the flexure compliance directions are mirror images of each other, a moment is induced about the vertical axis of the mirror. If the socket and clamps supported the mirror through its center of gravity, there would be no effect on the surface figure of the mirror. In actuality, this is not the case, and the moment causes the mirror to bend about the vertical axis. The surface is distorted cylindrically about this axis. This is the origin of the very strong astigmatism observed in the on edge test.

The presence of this astigmatism does not rule out "on edge" testing for a future SIRT mirror. It does require that the socket and clamp should pick up the load of the mirror through the center of

gravity of the mirror. This is difficult to achieve in a small mirror, due to the proximity of the center of gravity to the optical surface. In a larger mirror, it would not be a problem.

A plexiglass full-scale cross section model had been built for demonstration purposes, including the socket, clamp, and flexure. This model was placed between crossed polarizers and the screw holding the clamp torqued. It was possible to observe the peak stress areas in the model using photoelastic effects.<sup>5</sup> Although no effort was made to qualitatively analyze these results, the general shape of the stress concentration agrees well with the finite element model developed in the "Engineering analysis report" of May 1983. Figure 16 is a photo of the photoelastic test. It may be noted that virtually no stress appears to propagate to the optical surface of the mirror, and that the peak stress is in the area immediately adjacent to the clamp/socket interface.

## V. CONCLUSION AND DISCUSSION

It has now been shown that it is feasible to make the sockets and flexures as earlier designed in the "Engineering analysis report" (May 1983). It has also been shown that the RMS figure error for the 20-in. diameter double arch mirror and mount system can be on the order of 0.02 waves. The "on edge" test indicates that without a mounting system that picks up the mirror through its center of gravity, figure errors will remain very large, at an RMS of 0.45 waves. The simulation of cryogenic



Fig. 16. Photoelastic model of clamp and socket.

contraction of the baseplate did not produce a measurable change in the figure of the mirror. Without a higher resolution optical tests, the performance of the mirror and mount system can be guaranteed only to  $0.02 \pm 0.02$  waves.

It is suggested that the next experiment should be cryogenic testing of the mirror and mount system in the NASA Ames cryostat. Should test data be as ambivalent as the room temperature data, steps should be taken to perform testing with a higher resolution interferometer.

A high-resolution interferometer has been developed at the Optical Sciences Center for optical testing and has merit for this application. This device is called a Real Time Interferometer (RTI). The RTI uses a CCD array to record the interference fringes at a very short exposure time, typically on the order of milliseconds. The RTI interfaces with a computer; which is provided with a version of FRINGE. The computer is capable of storing and analyzing up to ten interferograms. This allows for removal of the effects of turbulence and vibration. In addition, stored error sources (such as auxiliary folding mirrors) may be removed at the same time. Current RTI technology reduces the interferogram error to about 0.005 waves. This is of the same order of magnitude as the figure change during cool down predicted by finite element methods.



It is suggested that following testing at NASA Ames, the mirror and mount be returned to the Optical Sciences Center for further room-temperature testing using the RTI. This would permit a better evaluation of the simulation technique, and a closer look at the behavior of the mounting system.

Another area of suggested future research is socket stress. The glass block containing the practice socket would allow photoelastic studies on clamping stress to be performed at both room and cryogenic temperatures. This would involve either removing a clamp from the mirror or fabricating a new one. In addition, a test to destruction could be performed on this glass block to see if the clamp system held up as well as the finite element model predicted.

A major unknown at this time is the stability of the aluminum baseplate at cryogenic temperatures. The "Engineering analysis report" of May 1983 detailed the effect of baseplate tilt on the performance of the mirror. Further development of this mounting concept will require information on baseplate behavior. Although it is possible to reduce the order of magnitude possible distortion by stress relief of the baseplate, this is not a totally adequate substitute for accurate information. It is suggested that a holographic test on the baseplate be performed at cryogenic temperatures; an inexpensive liquid nitrogen soak would probably yield meaningful information. Alternately, three flats could be located at the same point of attachment as the three flexures, and the tilt of the flats monitored as the temperature was lowered.

Should baseplate deformation prove a problem, a back-up design has been developed to reduce the order of magnitude of the effect of the mirror. This design would use a two-axis flexural gimbal ring to reduce moments transferred to the mirror. Commercially developed Bendix flex pivots would be used in the gimbal pivots. These flex pivots have a history of space use and represent a low risk (Fig. 17).<sup>6</sup>

ORIGINAL 17-319  
OF POOR QUALITY

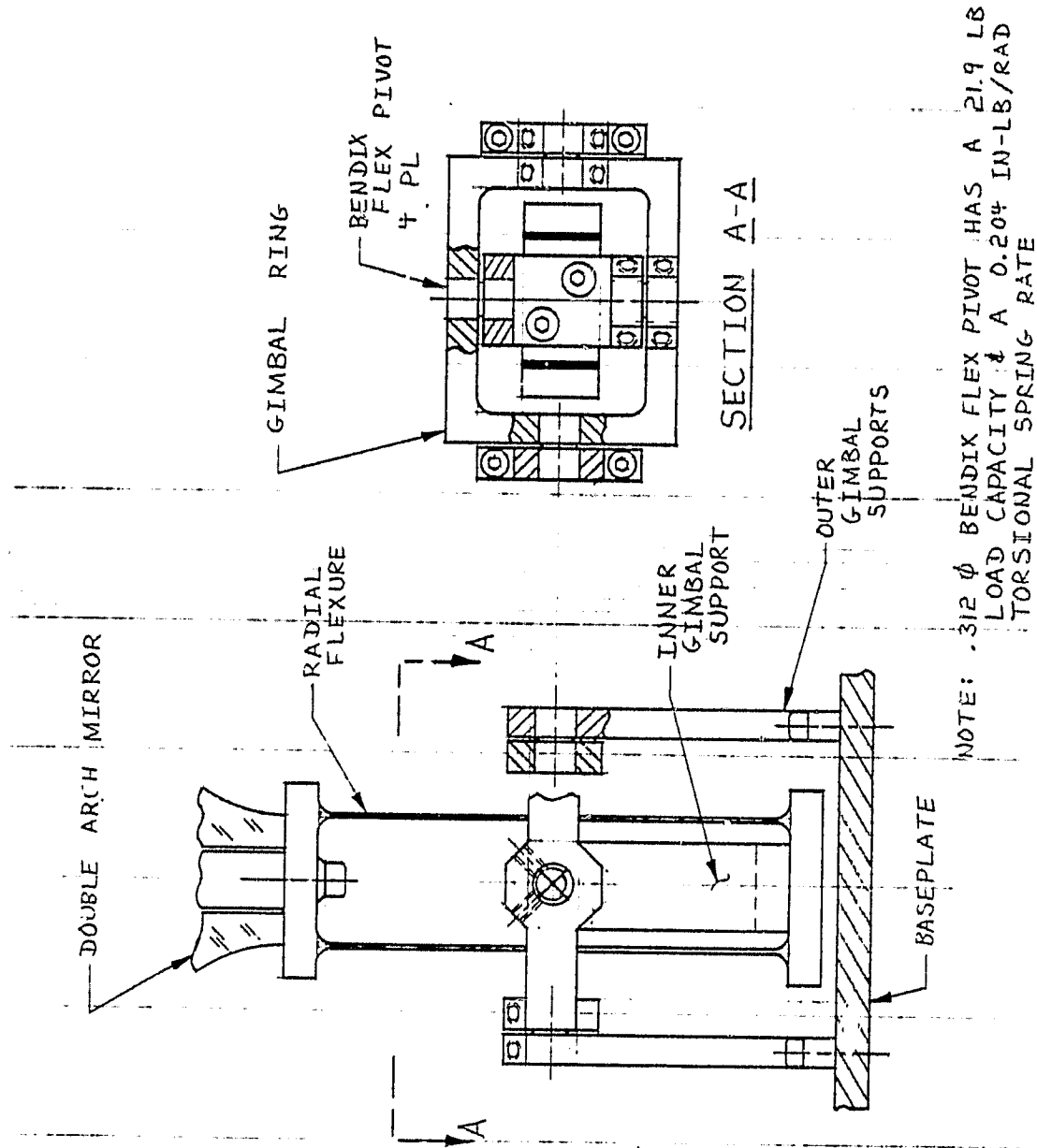


Fig. 17. Flexure gimbal system to reduce moments induced in the mirror due to baseplate deformation.

#### REFERENCES

1. Vukobratovich, D., et al., "Optimum Shapes for Lightweighted Mirrors," Proc. SPIE 332, 1982.
2. Anderson, D., et al., "Gravity Deflections of Lightweighted Mirrors," Proc. SPIE 332, 1982.
3. Republic Steel, Precipitation Hardenable Stainless Steels, Cleveland, OH, 1977.
4. Campbell, J. E., et al., Application of Fracture Mechanics for Selection of Metallic Structural Materials, American Society for metals, Metals Park, OH, 1982.
5. Haywood, R. B., Photoelasticity for Designers, Pergamon Press, Oxford, NY, 1969.
6. Seelig, E., "Flexural Pivots for Space Applications," presented at Third Aerospace Mechanism Symposium, Jet Propulsion Laboratories, Pasadena, CA, May, 1968.
7. Nelson, J. E., et al., "Telescope Mirror Supports: Plate Deflections on Point Supports," Proc. SPIE 332, 1982.

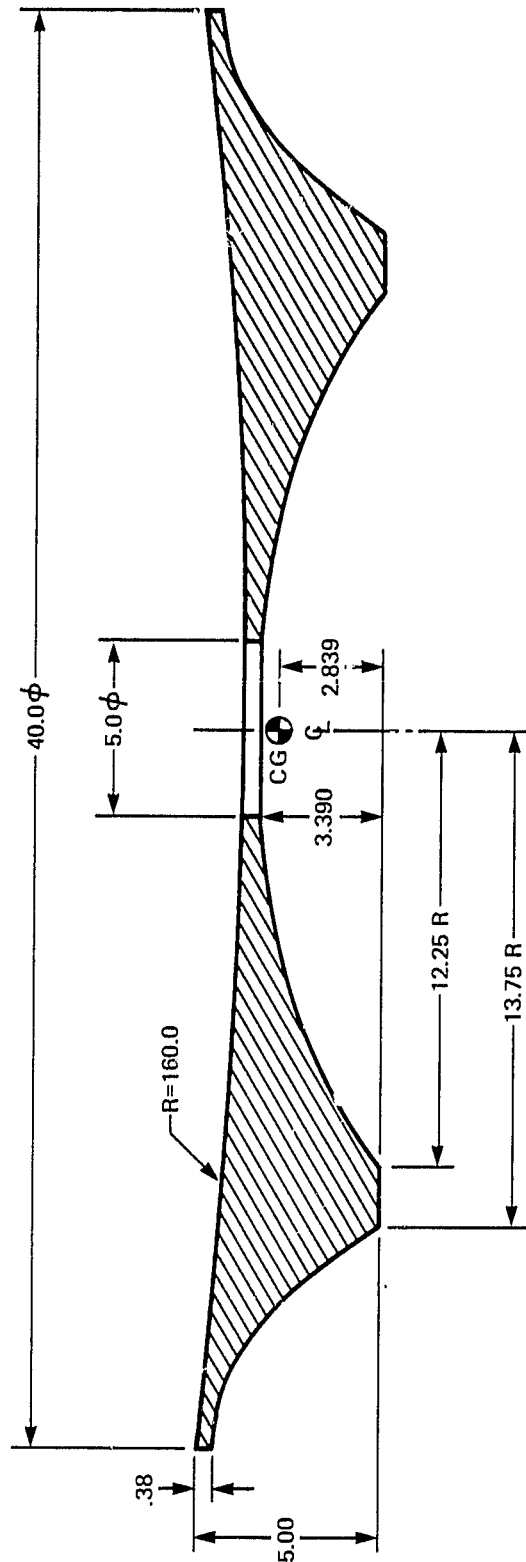
## APPENDIX:

### A PROPOSED 40-IN. DIAMETER PRIMARY MIRROR AND MOUNT FOR SIRTf

Using the technology developed in this contract, a 40 in.-diameter mirror and mount design was examined as a possible candidate for the SIRTf primary mirror. Two goals of the design were to hold the weight to the absolute minimum and to reduce self-weight induced deflection in a 1-G environment. The latter requirement is to ease the task of ground testing.

The 40-in. diameter mirror is a double arch design. It has a minimum thickness of 0.375 in. and a maximum thickness of 5.0 in. A speed of  $f/2$  was assumed; a second assumption was a 5.0-in. diameter center hole. If fabricated from Corning Code 7940 fused silica, the mirror would weigh 197 lbs (Fig. 18).

It is interesting to compare this design with other lightweight mirror designs. Such a comparison is facilitated by assuming that the weight scales as the cube of the diameter. A 36-in. diameter double arch has been fabricated for the Spacelab ultraviolet telescope. This mirror was an  $f/2$  and weighed 220 lbs. Scaled to 40-in. diameter, it would weigh 302 lbs. The MMT mirrors were 72-in. diameter fused-silica "egg-crates" and weighed 1200 lbs. If these mirrors were scaled to 40 in. diameter, they would weigh 206 lbs. State of the art today are the Teal Ruby and Space Telescope mirrors. The Teal Ruby mirror diameter is 20



**40"  $\phi$  f/2 NASA AMES SIRTf PRIMARY MIRROR**

VOLUME: 2461 IN<sup>3</sup>

WEIGHT: 197 LBS (FUSED SILICA,  $\rho=0.08$  LBS/IN<sup>3</sup>)

SURFACE AREA: 2754 IN<sup>2</sup>

Fig. 18. Proposed 40 in. diameter SIRTf primary mirror.

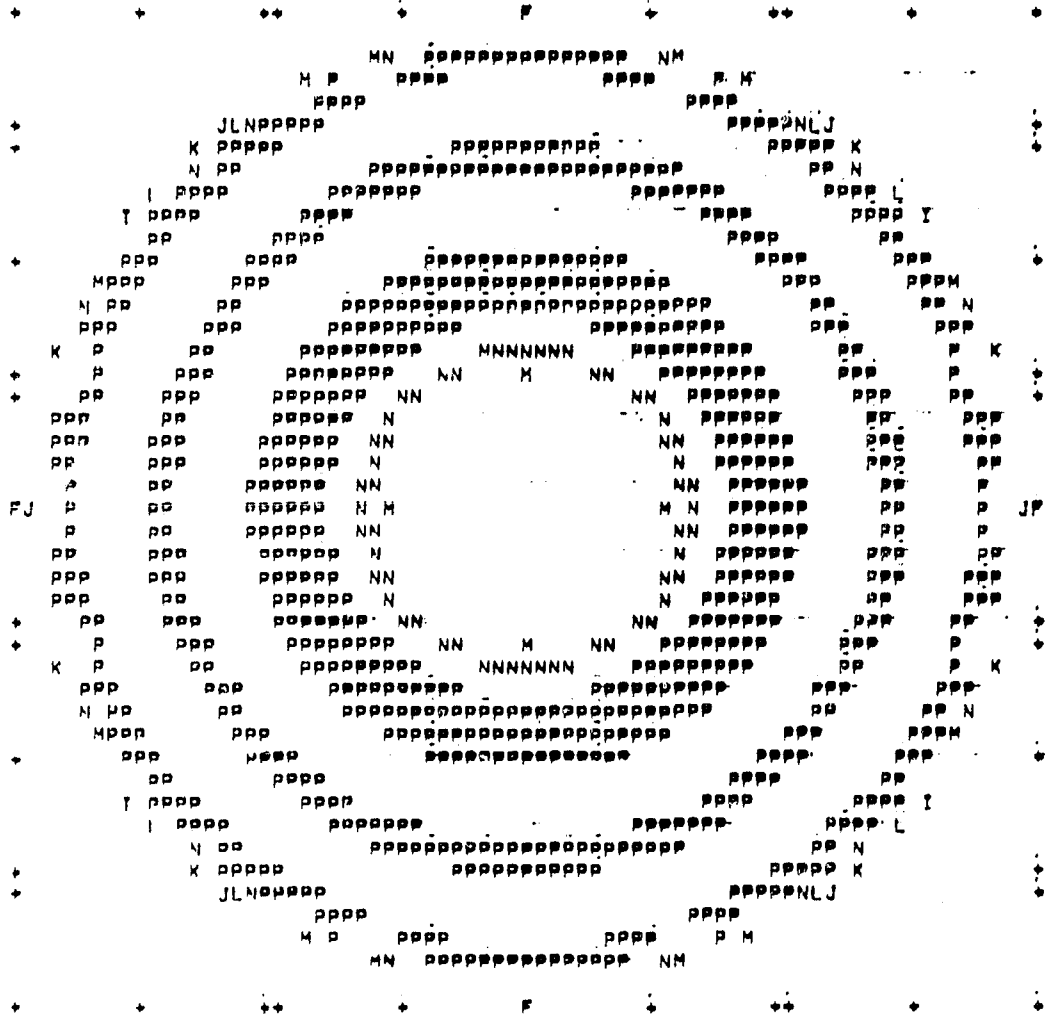
in., the mirror weight is 16 lbs. Scaled to 40-in. diameter, it would weigh 128 lbs. The Space Telescope mirror has a 98 in. diameter and weighs 1850 lbs. Scaled to 40-in. diameter, it would weigh 126 lbs. This suggested that the double arch design presented here is competitive with relatively conservative lightweight mirrors, but that it is substantially heavier than state-of-the-art designs. On the other hand, the double arch design is relatively simple to fabricate and can be quickly obtained. Arching of the double arch between supports, cutting relief pockets in the back, and further shape optimization may allow the weight to be reduced below 175 lbs. This would entail greater cost in time, risk, and dollars.

Reduction of self-weight deflection caused another look at the mirror's behavior. The greatest deflection is due to azimuthal sag between the three support points. Obviously, a continuous ring support would eliminate this. While a ring support is practical for shop testing, it would not be workable in a flight system. It is possible to closely approach the support efficiency of a ring by going to six support points instead of three.<sup>7</sup> A finite element model of the 40-in. double arch mirror on six points was analyzed. The predicted self-weight deflection in a 1-G field is seen in Fig. 19. The RMS deflection is 0.064 waves at 0.6328  $\mu$ M. The peak-to-valley error is 0.374 waves.

The six-point support system could be developed out of the technology that has been established in this contract. The support

ORIGINAL PAGE IS  
OF POOR QUALITY

<u>Contour step</u>	<u>Width</u>	<u>Page Size</u>	<u>-M-</u>	<u>-N-</u>	<u>-P-</u>	<u>-Q-</u>
1.000	0.500	2.000	-1.500	-0.500	0.500	1.500



Residual wavefront variations over uniform mesh:

<u>PTS</u>	<u>RMS</u>	<u>Max.</u>	<u>Min.</u>	<u>Span</u>	<u>Volume</u>
664.0	1.585	1.003	-8.325	9.328	24.568

Units =  $10^{-6}$  in.

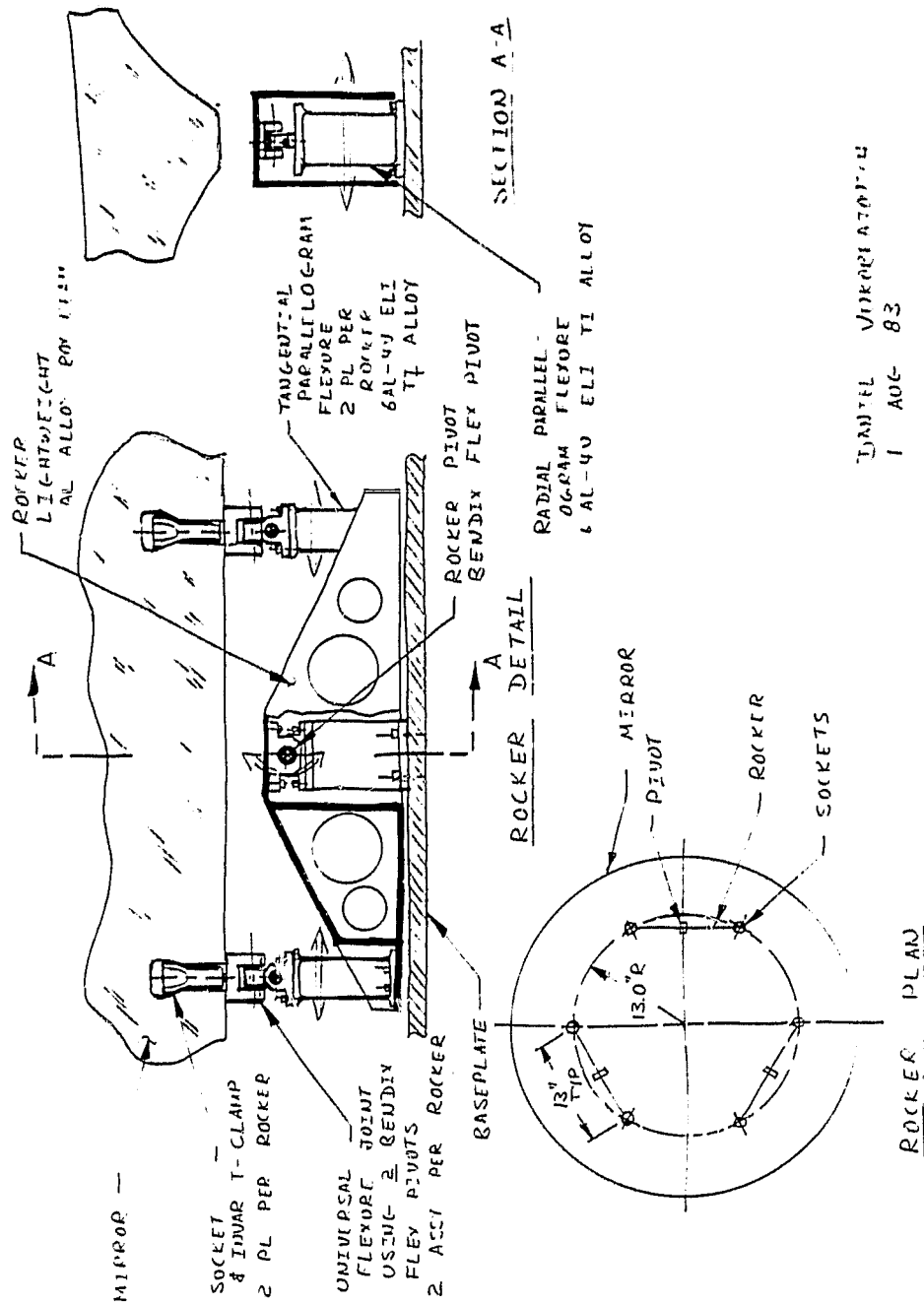
Fig. 19. Self-weighted deflection of proposed 40 in. SIRT mirror, mirror axis vertical.



system would use three rockers, the rockers mating to T-clamp/sockets at both ends of the rocker arms. A flexure system would tie the center of each rocker to the baseplate. This central flexure system would consist of a parallelogram flexure to remove radial contraction of the baseplate and a Bendix flex pivot to allow the rocker to tilt. A parallelogram flexure at each end of the rocker would take out contraction of the rocker arm relative to the mirror. A universal joint using Bendix flex pivots would couple the rocker arms to the T-clamp in the mirror back. This arrangement would virtually eliminate the baseplate tilt problem (Fig. 20).

It should be emphasized that this is a relatively conservative design that exploits existing technology. It would be possible to test the configuration on the existing 20-in. diameter double arch by adding additional sockets to its back. Fabrication time for the full size 40-in. mirror has been estimated to be about nine months.

ORIGINAL DRAWING  
OF POOR QUALITY



UNIVERSAL  
1 AUG 83

Fig. 20. Mirror mount details of six point support for proposed SIRT primary mirror.